Adsorption Phenomenon for Removal of Pb(II) via Teff Straw based Activated Carbon Prepared by Microwave-Assisted Pyrolysis: Process Modelling, Statistical Optimisation, Isotherm, Kinetics, and Thermodynamic Studies

Surafel Mustefa Beyan, Temesgen Abeto Ambio, Venkatesa Prabhu Sundramurthy, Chinnasamy Gomadurai & Abraham A. Getahun

View supplementary material

Published online: 24 Jan 2022.

Submit your article to this journal

View related articles

View Crossmark data

Taylor & Francis
Taylor & Francis Group

Check for updates

Adsorption Phenomenon for Removal of Pb(II) via Teff Straw based Activated Carbon Prepared by Microwave-Assisted Pyrolysis: Process Modelling, Statistical Optimisation, Isotherm, Kinetics, and Thermodynamic Studies

Surafel Mustefa Beyan [ID][a], Temesgen Abeto Ambio[a],
Venkatesa Prabhu Sundramurthy[b], Chinnasamy Gomadurai[c]
and Abraham A. Getahun[d]

[a]School of Chemical Engineering, Jimma Institute of Technology, Jimma University, Ethiopia; [b]Center of Excellence for Bioprocess and Biotechnology, Department of Chemical Engineering, College of Biological and Chemical Engineering, Addis Ababa Science and Technology University, Addis Ababa, Ethiopia; [c]Department of Chemical Engineering, Kongu Engineering College, Erode, India; [d]Central Laboratory, Research and Technology Transfer, Addis Ababa Science and Technology University, Addis Ababa, Ethiopia

ABSTRACT

*Eragrostis tef (*Teff) is one of the most important staple crops in Ethiopia. The straw obtained from teff is a plentiful source of lignocellulosic biomass. In the present study, straw obtained from teff grass was exploited as a carbon precursor to synthesise the activated carbon via chemical activation followed by microwave-aided pyrolysis. The prepared activated carbon by microwave aided method from teff straw (MATSAC) was utilised as a bio-adsorbent to examine the lead II ions adsorption potential from the aqueous medium. RSM technique was employed to explore a process model which correlates the four independent variables namely Pb(II) ions initial concentration, MATSAC dose, adsorption time, and solution pH. Further, the model was statistically optimised to achieve optimum Pb(II) ions removal. They were discovered to be Pb(II) ions initial concentration: 94.35 mg/L, MATSAC dose: 0.655 g/100 mL, adsorption time: 87.6 min, and solution pH: 5.4 to achieve the maximised removal of Pb(II) (90.89%). In the investigation on the models of isotherm, it was inferred that Langmuir isotherm fitted excellently to the equilibrium data of the adsorption. The adsorption capacity of Pb(II) on MATSAC was 42.97 mg/g. In addition, the kinetic analysis confirmed that the process of adsorption was statistically significant to pseudo 2nd order. The thermodynamic study indicated that the negative value of ΔG^{o} deep-rooted the practicability and spontaneity of MATSAC for Pb(II) ions removal. In a nutshell, MATSAC, which is derived from locally available agricultural waste, can remove toxic Pb(II) ions from contaminated water at a minimal cost.

1. Introductions

Accessibility of drinkable and safe water is more than likely to decrease very fast in the near future because of the increasing human-caused contaminants from industrial, domestic, and agricultural usage of water [1]. According to the 2017 UNESCO report, more than 80% of effluent is discarded into the environment without sufficient treatment across the world. This report also stated that the percentage of wastewater generation in developing countries reaches up to 95% [1]. Pollution of water is in dangering the natural water like rivers of different continent, mainly in Africa, Latin America, and Asia. About 800,000 deaths globally occurred in 2012, because of drinking water contamination and inappropriate hygiene services [1]. The main point of origin of these contaminates arises from different processing industries such as paint, tannery, batteries, and other refining industries. From different heavy metal pollutants, the most hazardous environmental pollution is caused by lead (Pb(II)) due to its various effects on human beings such as gastrointestinal illnesses, central nervous system damage, diarrhoea, and dizziness [2]. The degree of toxicity of lead has been examined in several investigations, for example, Microtox Assay has been used to measure the level of toxicity lead causes compared to other metals and the study reported as the order of the following: arsenic < cadmium < lead < mercury [3]. The maximum amount of Pb ions permitted in drinkable water is 0.05 mg/L [4]. In order to treat the wastewater contaminated by Pb(II), it is obligatory to apply different wastewater treatment techniques namely ion exchange, filtration, precipitation by chemical, coagulation, osmosis, membrane separation, and adsorption, among others.

Alternatives in a wide variety for heavy metal elimination, for instance lead, are very limited due to low efficiency, expansivity, complexity, and low selectivity [5]. However, because of its high efficiency and cheap cost, the adsorption method is recognised to be an effective technology for the uptake of various metals [6,7]. Here, the most fundamental aspect is adsorbent selection affording to the anticipated application. Different adsorbents have been studied to advance the adsorption, selectivity, reusability, and capacity for removals of a wide variety of heavy metals [8,9]. So far, several kinds of agricultural waste-based adsorbents, such as sugarcane bagasse, peanut shell, Arundinaria alpina, coffee husk, cellulose, and lignocellulosic-based material, woods (poplar and walnut), etc., have been used for treatments of wastewater [6–8,10–13]. The valorisation of these agricultural waste via preparing green-based absorbent chemicals epitomises an excellent solution to solve both of the environmental problems by one stone, meaning reducing solid agricultural waste as well as treatment of wastewater via the prepared adsorbent from the agricultural residue. Further, various nanoparticles [14,15], nanocomposites [16] and strains of yeast [17] have been used for the development of adsorbents.

Several numbers of materials have been as well examined for Pb(II) adsorption from contaminated water employing the adsorption method. Yosef Asrat et al. studied the utilisation of activated carbon (AC) adsorbent developed from Arundinaria alpina for the adsorption of Pb(II) ions from the synthetic media [6]. The authors reported that at the optimal process parameters 99.8% of Pb(II) was removed. An adsorbent developed from pomegranate wood was utilised for the removal of Cu(II) from wastewater [18].

Other studies choose agricultural biomass as the major precursors for the manufacturing of adsorbents intended for Pb(II) ions uptake from waste effluent; for instance, these authors developed adsorbents from the seed of avocado to take up chromium and lead from the solution of aqueous. They analysed the natural form and chemically activated form of the adsorbent and stated that, at operating parameters of pH (5) and temperature (25°C), the removal efficiency was greater than 80% [19]. Different authors reported the usage of different agricultural residues for preparations of green-based AC and utilised it for uptake of Pb from the water media. Nerveless, no research has been done on the utilisation of teff straw (agricultural residues) based green adsorbent for the adsorption of Pb (II) ions.

Teff straw (TS) is an abundant and native lignocellulosic waste in Ethiopia and found as a remaining waste after seeds were detached from the teff plant (*Eragrostis teff*) [20,21]. Globally Ethiopia harvest teff plant in the largest quantity, and it accounts for approximately 25% of all harvested crop product in 2017. After the seed of the teff is removed from the plant, the straw is discarded as agricultural waste [20]. This kind of lignocellulosic substance has no value for commercial purposes and signifies only alarming solid waste to the environment; hence, the development of green-based activated carbon/adsorbent from this kind of agricultural waste must be cheaper than adsorbent made from expensive precursors. Thus, this study's novelty lies in the preparation of green-based activated carbon and to recommend remediation for wastewater founded on this adsorption removal technology.

In the present study, emphasis has been given to synthesis the activated carbon using locally available, chemically activated plant biomass, teff straw, which is endemic to Ethiopia via microwave pyrolysis method; the microwave-based method of preparation of AC has been proven to be an effective technique for enhanced adsorption capacity [22] and characterise it. Further, the adsorption potential of prepared activated carbon (MATSAC) was investigated for the removal of Pb(II) ions from the synthetic solution by batch experiments. In order to maximise the Pb(II) removal, four independent variables, namely, initial concentration of Pb(II) ions, activated carbon dosage, adsorption time, and solution pH were considered and statistically optimised using the CCD-based RSM approach. Furthermore, the adsorption data were subjected to evaluate the adsorption kinetics, models of isotherms, and thermodynamic parameters. In addition, the reusability of bio-adsorbent was investigated by desorption and regeneration experiments.

2. Materials and methods

2.1. Materials

TS was found from agricultural land after the teff seeds are removed in Addis Ababa, Ethiopia. The TS was first rinsed several times using tap water to remove impurities and dust, and next via deionised water; next dried in the oven at 65°C for 2 days. Then, it was mashed and sieved to get the size of the particle, which is desired for this study. Analytical grades of zinc chloride ($ZnCl_2$), potassium nitrate (KNO_3), sodium chloride (NaCl), lead nitrate $Pb(NO_3)_2$, and distilled water was used for this study. For pH adjustment, sodium hydroxide (NaOH) and hydrochloric acid (HCl) were used. A standard solution (1 g/L) of

Pb(II) ions was set via Pb(NO$_3$)$_2$ (8 g) in distilled water (5 L). An Atomic Absorption Spectrometer (PerkinElmer, Model-PINAACLE 900 T) was utilised to measure the concentration of lead II ions by adopting the standard procedure.

2.2. Activated carbon adsorbent preparation

The AC adsorbent was synthesised from pyrolysis of the microwave process with the ratio of impregnation one-to-one (ZnCl$_2$ to TS) following the procedure of [23]. To create a smooth paste, the mixture was put into 0.05 L of pure water. The resulted paste was put in a quartz reactor under inert N$_2$ gas with a 2.5 mL/sec flow rate. This quartz device was inserted in the microwave for 5 min at 1300 W. The pyrolysed sample was then chilled using inert N$_2$ at a flow rate of 2.5 ml/sec. Subsequently, the carbonised substance was marinated with HCl: distilled water (1:1) solution at a temperature of 85°C for 120 min. This was done in order to leach out inorganic compounds from the sample matrix [24]. Till the washing water reaches a pH of 7, the carbonaceous material is washed excessively with distilled water. Afterwards, it was dried in the oven with continuous air supply at a temperature of 85°C for 12 hr. Finally, the AC developed from TS via the process of microwave-assisted pyrolysis was pulverised and sieved to the size of particle lower than 60 μm and it was named as MATSAC.

2.3. Characterisation of MATSAC

The product was characterised physically and chemically in order to test its compositions. To that end, the American Society for Testing and Materials (ASTM) methods were employed. Further, in order to measure the point zero charge (P$_{ZC}$) the subsequent assessment technique was adopted; 0.5 L of KNO$_3$ (0.1 N) in the 2 to 10 pH range was made ready in five different volumetric flasks. From the solution of NaCl (0.5 L), 45 ml was taken. Next, through adding a drop of HCl (0.5 N) and NaOH (0.5 N) the initial pH of the solution was adjusted, and then one gram of MATSAC was added to each volumetric flask and agitated for 2 days at 27°C. To this end, the pH was measured. The triplicate experiment was executed. The total charge that was absorbed on the surface of MATSAC was measured by calculating the pH difference (ΔpH) between 48 hr and initial pH. Then, the values of pH versus ΔpH were plotted and the point of intersection was used as a reference for measuring the P$_{ZC}$ value of the MATSAC.

The morphological characteristics of MATSAC were investigated using an SEM (FEI, INSPCT-F50, and Germany). The MATSAC was plated on stubs of aluminium, coated with tape made of carbon conductive material and imaged via SEM at 20.00 kV, 30 μm distance in a vacuum, and used for identifying the formation of porosity and surface morphology of MATSAC.

The specific surface area of MATSAC was analysed employing Brunauer, Emmett, and Teller (BET SA-9600, USA) techniques. This method adopted monolayer adsorption and then inert nitrogen gas desorption at a 77 kelvin through melting point analysis. For inert N$_2$ gas (2.5 bar) carrier and purging air to the surrounding, helium gas at a pressure of 2 bar was employed. Before analysing, MATSAC was pretreated at a temperature of 150°C for 60 min.

The prepared MATSAC was utilised for FTIR analysis to examine functional groups of the AC adsorbent. FTIR analysis was done between 4000 and 400 cm^{-1} wavenumber range. FTIR analysis was carried out using the KBr pellet method.

XRD (Olympus BTX^{TM}-528) examination was carried out via Cu–Co through a source of radiation (30 kV and 10 W) with an angle of diffraction (2θ) of 10° to 80°. The value of the threshold for splitting was four. The crystallinity from XRD information was obtained by employing the Scherrer Equation (1) with the aid of Origin 2018b pro software.

$$\text{Crystallinity} = \frac{\text{Crystalline peaks area}}{\text{All peaks area (amorphous + crystalline)}} \times 100 \qquad (1)$$

2.4. Pb (II) adsorption by MATSAC using RSM

The process of adsorption is significantly affected via more than a few variables, namely, adsorbent dosage, the adsorption process temperature, stirring, adsorbent particle size, contact time, and pH of the media, among others [7,25]. A preceding investigation was made by several researchers, who have proposed the optimum working condition for the uptake of Pb(II) ions onto the biomasses, which is selected [5,26–28]. To this end, adsorption analysis was done on a batch base to investigate the consequence of initial Pb(II) ions concentration, pH, adsorption time, and MATSAC quantity on Pb(II) adsorption efficacy of MATSAC.

A conical beaker containing 0.1 L of the sample was mixed via a thermostatic stirrer at room temperature and 200 rpm for each experiment run. Next, the solution was sieved via means of filter paper (Whatman No. 1), and the clear liquid was investigated for concentration of residue Pb(II) ion by AAS at 217 nm, and for each sample analysis, a blank solution was measured. Next, the adsorption efficiency of MATSAC was carried out (Equation (2)), and the adsorption capacity (Q) was calculated using Equation (3).

$$\text{Removal Efficiency (\%)} = \frac{C_o - C_f}{C_o} \times 100 \qquad (2)$$

$$Q\left(\frac{mg}{g}\right) = \frac{C_o - C_f}{m} \times V \qquad (3)$$

where, C_o (mg/L) and C_f (mg/L) are the concentrations of Pb(II) initially and at a given time t, respectively, m (g) denotes adsorbent mass and V (mL) denotes the adsorbate volume solution.

An investigation was conducted to optimise the adsorption efficacy of MATSAC and examine the collaboration effects of MATSAC dosage, adsorption time, pH, and Pb(II), on the removal effectiveness of lead from the synthetic solution via MATSAC. Other influencing parameters (agitation speed: 200 rpm at room temperature) were fixed as constant. For RSM investigation, the grouping of the chosen variables was engaged employing the central composite design approach (CCD). It warrants that each factor and the effects of their relationships are methodically investigated. The selected variables and their corresponding level are tabulated in Table S1. Grounding on the figure of constraints, CCD proposed a grouping of 30 experiments that justifies axial, factorial, and average levels. Thus, each experiment was studied three times, and the average value of (Pb(II)) result

after the adsorption was recorded. The obtained remarks found from the CCD experiments were statistically investigated by the variance of analysis (ANOVA) and fitted to a polynomial equation for developing a mathematical model to deliver the association among the response of the experiment and parameters. The polynomial equation is described is given in Equation (4)

$$R = \theta_0 + \sum_{j=1}^{4} \theta_j Y_j + \sum_{j=1}^{4} \theta_{jj} Y_j^2 + \sum_{i} \sum_{<j=2}^{4} \theta_{ji} Y_i Y_j + e_i \tag{4}$$

Where, R is the response [Pb(II) removal (%)]; Y_i and Y_j refer variables (i and j range from 1 to k); θ_0 refer to the coefficient of intercept; θ_j, θ_{jj} and θ_{ij} are known to be coefficients of interaction for the variables, respectively; and e_i is known as error.

Additionally, the process variables were optimised for the goal of maximising the Pb(II) removal using mathematical optimisation. Evaluations of all statistical constraints were achieved utilising ANOVA (analysis of variance). Through solving the equation regression of the chosen variables, the optimal values were found. The effects of interactions between the factors were investigated by conducting a response surface plot. RSM and CCD investigations were developed with the help of Design-Expert 12. For verification of the developed model, predicted by the design expert was proven through performing a triplicate experimental run.

2.5. Kinetics study

To accomplish the kinetic analysis, it was mixed 0.1 L of lead ions solution at 100 ppm with x g of MATSAC through continuously agitating at 250 rpm. Every five minutes aliquots were taken during the first half-hour due to the fast mechanism of adsorption before the saturation. Next, samples were taken every 60 minutes for 5 hr. The obtained data were adjusted to the models of kinetics (pseudo-first (Equation (5)) and second-order (Equation (6)) employing OriginPro 2018 software (OriginLab Corporation) to determine parameters of fittings and coefficient of correlation (R^2).

$$\log(q_e - q_t) = \log q_e - \frac{K_1}{2.303} t \tag{5}$$

$$\frac{t}{q_t} = \frac{1}{K_2 q_e^2} + \frac{t}{q_e} \tag{6}$$

where q_e is equilibrium adsorption capacity and q_t is at any time t, (mg/g) and K is pseudo constant for 1st and 2nd order.

The intraparticle diffusion kinetic model was considered to analyse using the Weber-Morris plot. It can be generated by q_t vs $t^{1/2}$, while the t is contact time. k_w is known as the intraparticle diffusion rate constant (Equation (7)). The use of this kinetic study can provide an idea of boundary layer thickness. This is accredited to the instant usage of the readily accessible absorbing spots on the surface of the adsorbent. The parameters C and kw were measured using the intercept and slope of the Weber-Morris plot's linear equation (Equation (7)). The model equation Elovich is an interesting model that can describe the activated chemisorption. In this model, a_e and b_e are known to be constants

that represent the initial rate of adsorption and surface coverage degree, respectively (Equation (8)). In addition, Bangham's model was utilised to determine the slow step that occurs in the MATSAC adsorption system. Where C_o refers to the Pb(II) ions' initial concentration in the media. V refers to the media volume and m is the of the adsorbent used per litre of solution. To determine the value of the parameter for k_B and α, the linear plot of log {log [(C_0/(C_0-q_tm)]} versus [logt] was generated and determined using slope and intercept (Equation (9)).

$$q_t = k_w t^{1/2} + C \tag{7}$$

$$q_t = [\frac{1}{b_e}\ln(a_e b_e)] + (1/b_e)\ln t \tag{8}$$

$$\log\left[log\left(\frac{C_o}{C_o - q_t m}\right)\right] = \log\left(\frac{K_o m}{2.303V}\right) + a\log t \tag{9}$$

2.6. Isotherm model study

The isothermal model was carried out for one day via varying Pb(II) initial concentration under fixed variables, which were found out from optimisation analysis. The Freundlich (Equation (10)) and Langmuir (Equation (11)) isotherms were designated in order to fit results from the experimental analysis, which is accomplished via the batch mode adsorption process.

$$\log q_e = \log K_f + \frac{1}{n}\log C_e \tag{10}$$

$$\frac{C_e}{q_e} = \frac{1}{bq_{max}} + \frac{C_e}{q_{max}} \tag{11}$$

where adsorption energy (b), the highest capacity of adsorption (q_{max}), quantity adsorbed per quantity of adsorbent at the conditions of equilibrium (q_e) (mg/g), equilibrium concentration (C_e) (mg/L), and capacity of adsorption (K_f) and intensity of adsorption (n).

2.7. Thermodynamic study

To analyse the thermodynamics property of the biosorption process of Pb(II) on the MATSAC, the parameters of thermodynamic property such as ΔH^0 (enthalpy change), ΔG^o (free energy change) and ΔS^o (entropy change) have resulted via Equations (12) and (13).

$$\Delta G^o = -RT\ln K_a \tag{12}$$

$$\ln K_a = \frac{\Delta H^o}{RT} + \frac{\Delta S^o}{R} \tag{13}$$

where R (8.314 J/mol. K) is a universal gas constant, $K_a \left(K_a = \frac{q_e}{C_e} \right) \left(\frac{L}{g} \right)$ denotes the coefficient of distribution, and T (K) denotes absolute temperature. Employing the relations (Equation (12)), ΔG^o was determined at different temperatures of the process such as 298, 303, 318, and 333 K. Equation (13) is recognised as Van't Hoff Equation that can be utilised to calculate ΔH^o and ΔS^o values. In these investigations, $lnK_a Vs 1/T$ plot will be used to determine ΔH^o (slope of the plot equation) and ΔS^o (intercept of the plot equation) values.

2.8. Studies on adsorbent desorption and regeneration

Bio adsorbent reusability can be studied via the desorption method. To see the sight, reverse activity for Pb(II) adsorption via MATSAC the batch modes adsorption process was employed. For the desorption investigation, different concentrations (1–10 mol/L) of HCl and HNO_3 were used in order to accomplish the process of regeneration. Accordingly, air-dried adsorbent (2 g) that was loaded with Pb(II) ions was used. MATSAC loaded with Pb(II) ions was inserted into a 250 mL flask containing 100 mL of desorbing eluents (HNO_3 and HCl). Next, the solution was continuously mixed in an orbital shaker at 27 °C with 120 rpm. The desorption process was carried out for both eluents that did not surpass 110 min. To this end, the efficacy of desorption (%) of lead II ions from solid phases of the MATSAC was determined employing Equation (14).

$$\text{Desorption Efficacy } (\%) = \frac{C_1}{C_2} \times 100\% \tag{14}$$

3. Results and discussions

3.1. MATSAC characterisations

An adsorption process is a complex event that encompasses numerous stages; thus, several constraints affect heavy metal removal efficiency from aqueous media. Table 1 presented the results of proximate analysis for MATSAC and different agricultural biomass. It was obtained that fixed carbon content is highest in the proximate analysis of the MATSAC. These outcomes were anticipated because of such element content in lignin, hemicellulose, and cellulose molecule [9]. Heavy metal removal using a material with high lignocellulosic composition is credited to the existence of functional groups, namely, amines, hydroxyl and carboxyl [6,7]. The moisture content (MC) of a substance is determined by the amount of vaporised water that it contains [29]. MATSAC is a porous

Table 1. Proximate and ultimate analysis of MATSAC and agriculturally based adsorbent.

Biomass	C (Mc/cm)	FCC (%)	CY (%)	HY (%)	MC (%)	AC (%)	VM (%)	BD (g/cm^3)	SA (m^2/g)	pH	P$_{ZC}$	References
MATSAC	0.61	69.74	65.18	4.62	5.78	5.03	18.42	0.76	494.2	7.15	4.86	Present work
EFB	-	67.66	68.32	3.12	7.53	9.58	15.23	-	720	-	-	[32]
MLA	-	69.14	64.90	-	4.12	5.43	21.31	-	-	6.95	-	[28]
HDAC	-	67.1	85.7	2.0	8.4	10.8	13.7	-	1359	7.25	-	[30]
RHC	-	-	-	-	13.8	38	-	0.68	105.4	6.5	-	[29]

where C is conductivity, FCC is fixed carbon content, CY is carbon yield, HY is hydrogen yield, MC is moisture content, AC is ash content, VM is volatile matter, BD is bulk density, SA is surface area and P$_{ZC}$ is point zero charge.

material that has lower MC, AC, and VM. The capacity of adsorption of the AC sample would be poor if AC is high, thus a high ash content is undesirable [28,30]. It contains fewer non-carbon components than its main carbon counterpart. The graphitisation grade of MATSAC properties can be claimed due to its higher percentage of FCC and CY [31,32]. The high percentage of CY and FCC of the MATSAC make it an excellent candidate for the production of an adsorbent. The FCC and CY of MATSAC are likewise pointedly more than those found in other lignocellulose-based ACs, such as corncob and coffee husk-based ACs [6,33]. The density of bulk (BD) had better not be exceeded 0.25 g/cm^3 to allow for the possibility of using agricultural waste adsorbent as activated carbon. The MATSAC has a bulk density of 0.79 g/cm3 as shown in Table 1, which meets the aforementioned requirement. The adsorbent surface charge, which is regulated by the medium pH, has the greatest impact on the charged Pb (II) ions of group adsorption onto the surface of MATSAC. According to Cruz-Lopes et al. [27], carbon pH in the range of 5.5 to 7.5 is acceptable for most adsorbents for removal of Cr^{6+}, Ni^{2+}, and Pb^{2+}. The relationship between P_{ZC} and adsorbent capacity (MATSAC) is that cation adsorption on any adsorbent will likely increase with P_{ZC} values lower than pH values, but anions adsorption will be favourable at PZC values greater than pH values [34].

MATSAC has a specific surface area of 494.2 m^2/g conferring to the attained result via the investigation of the BET instrument. This outcome established that the microwave-assisted pyrolysis technique formed porosity on the TS and made it a suitable AC for the uptake of heavy metal. Nevertheless, the obtained BET-specific surface area of MATSAC is relatively lesser than commercially obtainable AC [7]. This result is also reinforced by the MATSAC SEM morphology analysis (Figure S1).

The scanning electron microscope (SEM) has long been a valuable tool for determining the morphology of a surface and gaining insight into the adsorbent's physical properties and structure. The surface morphology of MATSAC is shown in Figure S1. The surface structure of the raw agricultural resides of teff straw was uneven and rough with no pores. However, many pores were discovered in the MATSAC due to the modification of the TS by an activating agent, which was produced using microwave-assisted pyrolysis method, for improved heterogeneous adsorption process is shown in Figure S1. A distinct appearance in the shape of cylinders that were agglomerated with each other was discovered for MATSAC (Figure S1). The lignocellulosic material was broken down at processing temperatures, followed by the volatile chemical evaporation, leaving the material with well-formed stomates. This surface porosity could be well thought out as a factor for heavy metal, Pb(II) ions, binding.

Fourier Transformed Infrared Spectroscopy (FTIR) was employed to investigate the functional group's presence that is responsible for lead ion adsorption on the adsorbent (MATSAC) materials surface; this method produces peaks that show various wavelengths that are directly related to the infrared radiation energies. The FTIR spectra of bio-adsorbent are shown in Figure S2. Due to the different detected bands, the complexity of lignocellulosic materials was confirmed. Several bands have been discovered at 3528 cm^{-1} (O-H stretching), 1977 cm^{-1} (C-H bending), 1611 cm^{-1} (C=C stretching), 1384 cm^{-1} (C-H bending) and 699.7 cm^{-1} (C=C bending). The bonds established among the active sites of the materials and the heavy metal ions could be linked to the adsorption phenomena [9].

The XRD tool was employed in order to explore the crystalline and amorphous structure of locally synthesised MATSAC (Figure S3). The absence of a strong peak indicates that the majority of the active areas have been covered with the amorphous nature of carbon, which in turn makes it an excellent adsorbent [35]. There is a broad diffraction background corresponding to a 2θ angle between 19.47° and 32° in the spectrum, which relates to an amorphous structure of MATSAC. A small peak corresponds to 2θ = 36.58°, 2θ = 43.19°, 2θ = 47.4° and 2θ = 48.48° in the spectrum are related to the crystalline structure of the adsorbent (MATSAC). A small signal indicates that the MATSAC is only partially graphitised and contains relatively fewer graphitic crystals [35]. The crystallinity measured by MATSAC is 12.76% with 87.24% structure of amorphous. The obtained result was very close to previously studied results of activated carbon that are synthesised using different precursors of legionellosis material [35,36].

3.2. Lead II ions adsorption using MATSAC and CCD modelling

3.2.1. Model analysis

Five levels were proposed, for each variable that affects the process of the adsorption, the basis on the maximum removal capacity from a batch-type adsorption conferring to previous work and one factor at a time approach [5,6,37]. The RSM-CCD technique was used to choose the most appropriate model for the process and to enhance the adsorption course parameters [38].

The interaction effect for the four designated variables, which are initial Pb(II) concentration (A), the dosage of MATSAC (B), pH of the solution (C), and contact/adsorption time (D), on the adsorption of Pb(II) ions was investigated with 30 randomly selected experimental runs which are designed by CCD method. The adsorbent, MATSAC, prepared using an agricultural waste, teff straw, has a removal capacity of lead II ions from the solution in the range of 16.56% to 92.59% (Table S2). The maximum difference between the actual experiment and the projected value by the model is insignificant, which supports the model and the actual experiment are in close agreement. This finding is consistent with earlier research on the removal of Pb(II) ions on different activated carbons made from agricultural waste [37,39–44]. Due to the quadratic model having maximum values of both predicted and adjusted R-square (0.9753 and 0.9319 respectively), it is selected (Table S3). As a result, the quadratic model's prediction success is the most appropriate for the current design (Equation (15)).

$$Pb(II)ions\ removal(\%) = +90.17 - 18.89A + 3.71B + 4.10C - 1.89D$$
$$- 0.8619AB + 6.10AC - 1.99AD - 2.28BC + 1.99BD \qquad (15)$$
$$- 2.20CD - 9.50A^2 - 2.82B^2 - 4.338C^2 - 10.05D^2$$

3.2.2. Analysis of variance

Table S4 shows the results of an ANOVA analysis conducted to examine the impact of each process variable and their overall significant interaction on the adsorption efficiency of MATSAC to Pb(II) ions from the solution medium. The model's terms will only be significant if the p-values are less than 0.05 [7]. A (initial Pb(II) ion concentration), B (MATSAC dose), C (adsorption time), D (solution pH), AC, AB, AD, BC, BD, CD, A^2, B^2,

C^2, and D^2 are model terms that are significant (p > 0.05) in the present studies (Table S4). This represents that the independent variables are noteworthy; thus, the selected parameters and their interaction effect influence the adsorption of Pb(II) ions by MATSAC. This discovery is also in pact with various previous researches which are carried out on AC developed from wastes of agriculture [45,46]. For Pb(II) ions removal from the solution, the model has a p-value > 0.0001 and the F-value is 82.65 (Table S4).

3.2.3. Parameter interaction effect analysis on the adsorption process

In this study, with the aid of the RSM-CCD technique, the substantial process variables specifically Pb(II) particles' initial concentration, MATSAC dosage, adsorption period, and solution pH, were examined on the adsorption effectiveness of Pb(II) ions. By putting the two independent process factors constant at their central level, the interaction effect of the other two factors on Pb(II) ions uptake was examined and given as follows below through 3D response surface schemes (Figure 1).

The adsorbent quantity and initial concentration of lead II ions interaction effect on adsorption of Pb(II) ions from the synthetic media were explored in the range of 40 ppm to 160 ppm and 0.2 to 1 g/100 mL, respectively (Figure 1(a)). The highest removal efficiency (92.89%) of the adsorbent (MATSAC) occurred at the initial Pb(II) ion concentration of 86.867 ppm and adsorbent dose of 0.473 g/100 mL, whereas the adsorption time and the solution pH were kept at the mean level. Accordingly, it can be seen that the reduction in initial concentration of Pb(II) ions and the rise in dosage of MATSAC has increased the adsorption process. This is because as the initial Pb(II) ions are low, the sites for adsorption and surface area of the MATSAC became more available of the ions attached to the void adsorbent surface area, increasing the adhesion of the molecule to the surface of the MATSAC. However, as lead molecule concentrations increased, the adsorption rate became slow as a result of the saturation of the binding sites and also rivalry among Pb(II) ions for the fewer number of available binding sites. In a pact with this study remarks, Khanniri et al. stated that the efficacy of removal of metal reduced with the increase in initial lead ion concentrations in aqueous media via adsorbent [43]. Greater than 80% of removal efficiency of Pb(II) ions was obtained when the initial metal concentration enlarged from 40 ppm to 80 ppm along with adsorbent dosage ranging from 0.2 to 0.8 g/100 mL. Above the optimal Pb(II) concentration, the active sites needed for the adsorption of the ions will be absent. This hinders the overall adsorption by the adsorbent. Similar studies were revealed by Bayuo et al. [47].

The interactive effect of initial Pb(II) ions concentration and adsorption time on Pb(II) ions adsorption by MATSAC was investigated in the range of 40 to 160 ppm and 50 to 110 min, respectively; their interaction effect was significant with the p-value of less than 0.0001. Adsorption efficiency of MATSAC was greater than 80% was obtained when the Pb(II) initial concentration was in the 40 to 100 ppm ranges and adsorption time was in the 30–90 min ranges, and the adsorbent dosage and the solution pH were at medium level. At adsorption time of 89 minutes and 88.7 ppm an initial concentration of ions, the highest uptake efficacy of lead (II) was 93.3%, with the adsorbent dosage and pH value adjusted to the centre level. Because of the low dissolved ions ratio to sites of the adsorbent, more ions may be coupled to the accessible surface area of MATSAC at a time with fewer levels of Pb(II) ions. At increasing levels of metal, however, the effectiveness of the adsorption process is reduced, most likely as a result of adsorption sites overload and fighting among the Pb (II) ions for a smaller quantity of available receptors. Founded on the data
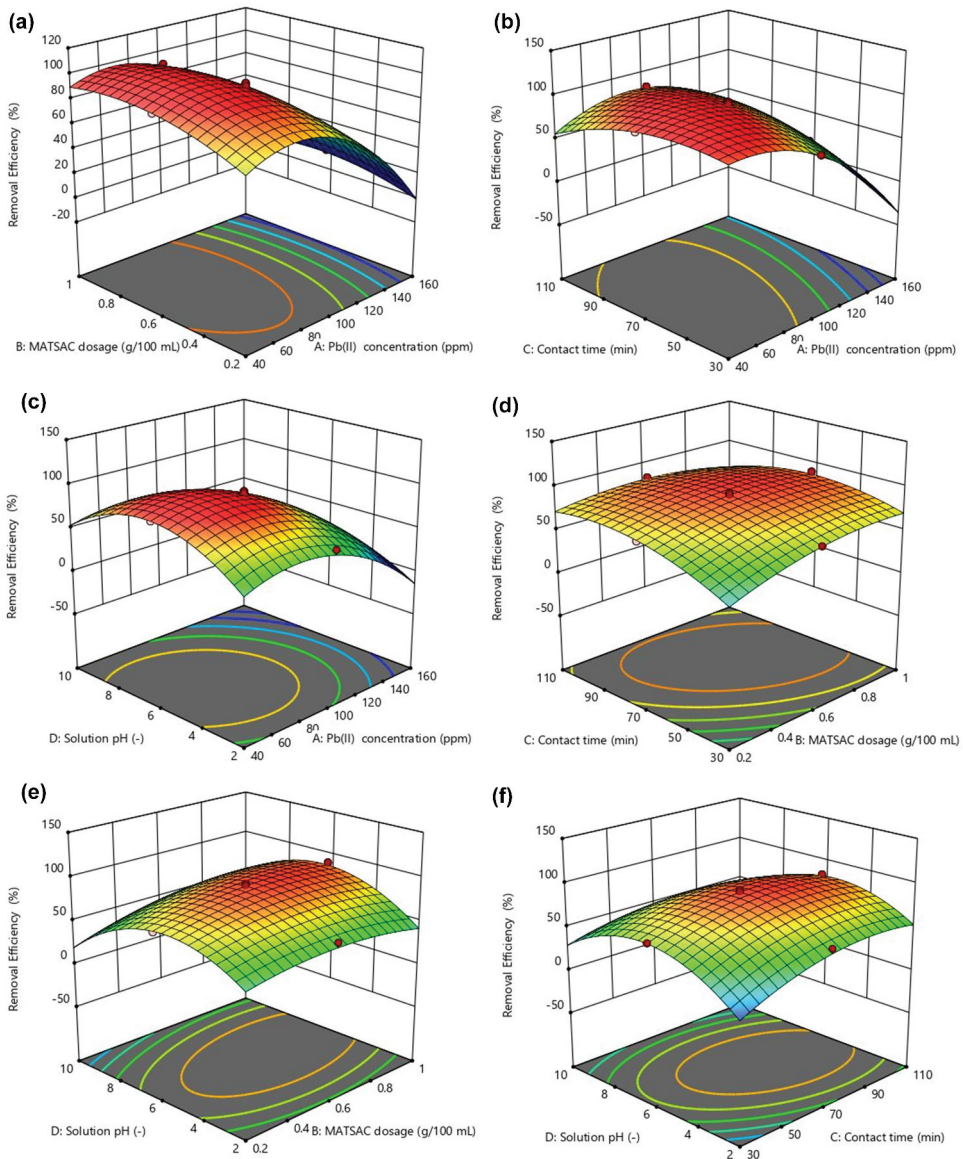
Figure 1. (a) interaction effect of, initial Pb(II) ions concentration and MATSAC dose, (b) initial Pb(II) ions concentration and contact time, (c) initial Pb(II) ions concentration and solution pH, (d) MATSAC dose and solution pH, (e) MATSAC dose and contact time and (f) solution pH and contact time on Pb(II) ions removal from aqueous media.

displayed in Figure 1(b), because there were adequate active sites accessible for adsorption, the adsorption rate was greater during the initial contact period. However, when the amount of Pb(II) ion adsorbed on the adsorbent surface increased over time, the surface area became completely occupied. Jonas Bayuo et al. developed a groundnut shell adsorbent for the Pb(II) ions uptake from synthetic media. They stated that an optimum time of 90 min was needed to obtain the highest removal efficiency of 90.26% and after this, the removal efficiency of the adsorbent was constant [47].

The interactive effect of initial Pb(II) ion concentration and solution pH from the 3D surface plot is depicted in Figure 1(c); the interaction effect on the removal of Pb(II) particles was obtained to be significant with the p-value of 0.0425 (Table S4). Changing the pH of heavy metal-containing solutions affects the surface charge of the adsorbent and the ionisation degree of the adsorbed heavy metal ion throughout the process of sorption [48,49]. As presented in Figure 1(c), the adsorption process of ions from the media enhanced with increasing the pH solution from 2 to 5.5. Nevertheless, the effectiveness of the adsorption process decreased at pH values less than and more than 5.5, resulting in the maximum adsorption of Pb(II) ions by MATSAC at pH 5.5 in aqueous media. The pH value of the solution influences the chemistry of lead(II) ions, its competition for available sites of adsorption, and the net charge of functional groups on the MATSAC surface, which may modify their ionic state. An anionic binding site which was accountable for competition among the Pb(II) ions and concentration of hydrogen ions in the media to be adsorbed in the active surface area of MATSAC at low pH results in increasing the charge density of the positive surface of the ligands [42]. As a result, the electrostatic interaction between adsorbent materials and the lead(II) ions was reduced. Conversely, the ability of adsorption reduced at high pH values due to the $Pb(OH)_2$ precipitates development and/or the hydroxo ion $Pb(OH)^+$ in the media, resulting in a drop in lead(II) concentration on the MATSAC surfaces [6]. Awual et al. reported similar results, stating that the solution pH from 2 to 8 was chosen to remove the Pb(II) ions from a synthetic media and that the high adsorption effectiveness of Pb(II) ions by adsorbent was reached in the solution pH of 5.2 [50].

The adsorption of Pb(II) ions by MATSAC as a function of adsorbent dosage and contact/adsorption time with the central value of initial Pb(II) ions concentration and solution pH is given in Figure 1(d). The interaction effect is obtained to be significant with a p-value of 0.0266. The obtained data exhibited that the adsorption process enhanced with a rising dosage of MATSAC from 0.2 to 0.8 g/100 mL and the adsorption time from 50 to 90 min. Figure 1(e) depicts the interaction effect of adsorbent quantity and solution pH in the removal process of Pb(II) ions. Their interaction effects are also found out to be significant with a p-value of 0.0432. Significant interaction (p-value = 0.0272) was also obtained for adsorption time and pH of the media for the adsorption process of lead from aqueous media (Figure 1(f)).

3.2.4. Parameter optimisation for optimum removal of Pb(II) ions

Triplicate tests were executed to determine the significance of optimisation outcome under optimal points projected by the CCD design model. The mean value of the observed (experimental) result of the removal efficacy of MATSAC at those optimal levels was in close pact with the predicted value of the model (Table 2). Thus, this validation proves the suitability of the quadratic model for this process.

We compared the maximal adsorption capabilities of our current MATSAC to the findings of other studies [39–41,44,51,52] utilising adsorbents from different sources of agricultural waste for Pb(II) ion adsorption. Table 3 tabulated that teff straw-based activated carbon had the acceptable potential (42.97 mg/g) for lead(II) ion adsorption among other agricultural waste-based AC.

Table 2. Optimal conditions of the selected factors for Pb(II) ions adsorption via MATSAC.

Process parameters	Initial Pb(II) concentration (ppm)	MATSAC dose (g/ 100 mL)	Adsorption time (min)	Solution pH	Removal efficiency (%)		Desirability
					Predicted	Actual	
Optimised conditions	94.355	0.655	87.631	5.4	92.96	90.89	1

Table 3. Adsorption capacities of Pb(II) ion comparison with various adsorbents.

| Adsorbent	Q_{max} (mg/g)	References
MATSAC	42.97	Current study
Meranti sawdust	34.25	[39]
Mentha piperita carbon	53.19	[40]
Solamen Vaillanti snail shell	26.04	[53]
Padinasanctae-crucis algae	80.64	[54]
Fig sawdust	80.64	[44]
Activated Carbon date pits	30.70	[51]
Peanut hull	30.43	[41]
Algal waste	44.00	[52]

3.3. Kinetic study

When it comes to adsorption, kinetic features should be considered to learn more about its performance and mechanics. The mechanism of a specific solute's adsorption on the material is somewhat complicated. The adsorption kinetics study is particularly valuable for both understanding the mechanisms involved and designing futures on large-scale adsorption facilities [44]. Several mathematical models for describing adsorption data have been presented in recent decades. In the current study, five kinetic models have been selected namely pseudo-1st-order, −2nd-order, intra-particle diffusion, Elovich and Bingham's model were employed to anticipate the mechanism at work in the current biosorption process.

3.3.1. Pseudo-first-order kinetic model

Lagergren proposed a pseudo-first-order equation (Equation (5)) which is founded on the solid capacity for the sorption of liquid/solid systems. Figure 2(a) depicts the linearised version of the pseudo-first-order kinetic model for the Pb(II) ion adsorption onto the MATSAC adsorbent. The slopes and intercepts of log(qe-qt) vs t plots were utilised to calculate the rate constant k1 and adsorption density qe, respectively, and they are listed in Table S5. The value for coefficients of correlation, R^2, this kinetic model was low, indicating a poor linearisation quality. This indicated that adsorption of Pb(II) ions diverged significantly from the pseudo-first-order kinetic model and may not be sufficient to describe the adsorption process of Pb(II) on MATSAC surfaces.

3.3.2. Pseudo-second-order-kinetic model

Mckay and Ho established a pseudo-second-order equation based on the amount of sorbed sorbate on the sorbent [55]. This equation has been used to effectively adsorb organic compounds, oils, metal ions, dyes, and herbicides from aqueous solutions
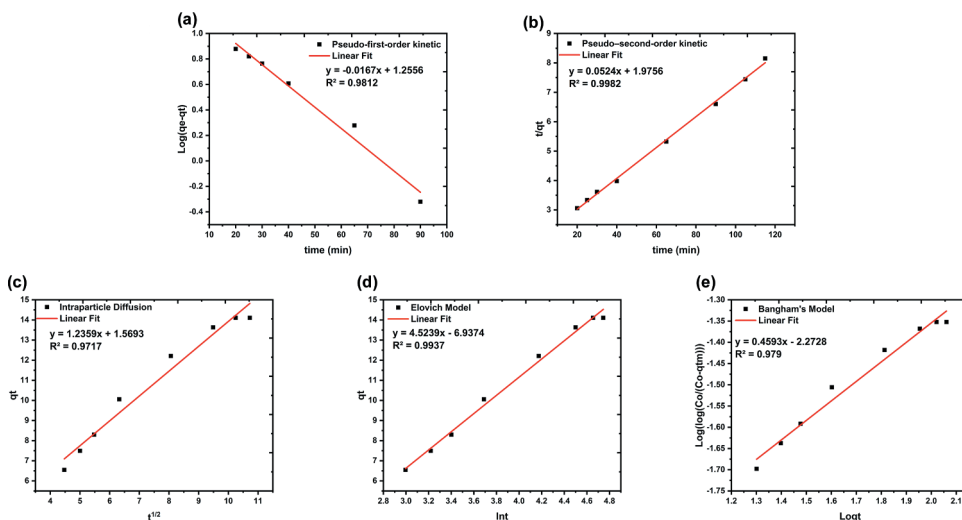
Figure 2. Fitting of adsorption data for (a) Pseudo-first-order, (b) Pseudo-second-order kinetic equations, (c) Intraparticle diffusion, (d), Elovich model, and (e) Bangham's model for removal of Pb(II) ions by MATSAC.

[6,56,57]. As depicted in Figure 2(b), the plots of t/qt vs t resulted in linearised graphs. The slope and intercept of the plot were used to calculate the values of the adsorption constraints, qe, and k2, respectively (Table S5). The R^2 value for this kinetic model was obtained to be 0.9982, demonstrating that the adsorption process analysed is a second-order kinetic model.

3.3.3. Intra-particle diffusion model

If a linear plot of qt against t1/2 passes through an origin, then intra-particle diffusion is the only rate-limiting step [58]. Figure 2(c), on the other hand, demonstrated that the linear plots did not go through the origin. Even though intra-particle diffusion played a role in the process of adsorption, it was not the only rate-determining step. The parameter values for this model are tabulated in Table S5.

3.3.4. Elovich model

The Elovich adsorption equation was created to describe the chemisorption kinetics of gases onto solids [39], which has lately acquired popularity for describing the kinetics of adsorbate adsorption onto adsorbents in the aqueous medium. To examine the adsorption kinetics using the Elovich model, a straight line of qt vs lnt should be drawn in order to determine the model constants a_e and b_e from the slope and intercept of the plot, respectively, which are provided in Table S5. The chemical relevance of these constants has yet to be determined [59]. Figure 2(d) depicts the Pb removal efficiency of MATSAC predicted by the Elovich kinetic model.

3.3.5. Bangham model

To examine the adsorption kinetics using the Bangham model, a logarithmic plot was depicted in Figure 2(e). The Bangham model's, $R^2 = 0.979$, indicated a convergence with linearity, indicating that tartrazine diffusion into the pores of the adsorbent was also the rate-controlling mechanism [60]. This indicates that both film diffusion and pore diffusion played a role in the adsorption process to varying degrees [60].

The computed q_{cal} values for metal ion sorption derived from the pseudo-2nd-order model were near to the data of the experimental, q_{exp}, values. It was obtained that the pseudo-second-order kinetic model best defined Pb(II) ions adsorption kinetics via MATSAC, grounding on the value of the correlation coefficient. The experimental data fitting to this model specified that the process of adsorption is governed by the chemical method because of the chemical bond created between the active site of the adsorbent and the adsorbate. Based on the estimated value for constant K_2, it is revealed that the initial adsorption rate for the ions by the MATSAC was also high, attaining high adsorption proficiency. The kinetic data analysis demonstrated that there was a multiple adsorption stages control for adsorption of Pb(II). A significant correlation coefficient was observed (0.979) for the Bangham model, which suggested that the pore diffusion was involved. However, the linearity of the plot generated by Bangham model explicated that Pb(II) pore diffusion was not the only rate controlling step. As per the profile obtained by intraparticle diffusion model, the data plot did not pass through the origin, which suggested that there was also a boundary layer diffusion for uptake of Pb(II). Based on the adsorption kinetics analysis, the Pb(II) heavy metal ion interaction with the MATSAC can be schematically represented as given in Figure S4.

Huang et al. prepared titanate nanoflower and studied their adsorption kinetics and isotherm for Pb(II) adsorption [61]. The authors discovered that pseudo-2nd order kinetic and Langmuir isotherm was suitable for fitting the experimental results. Researchers synthesised a low-cost and green-based, which is solid-phase activated carbon from the husks of coffee waste to absorb Pb(II) from the solution and investigated parameters' effect on the removal process. They discovered that the maximum removal was 98% and capacity of adsorption was 19 mg/g and the pseudo 2nd order kinetics model demonstrated the best fitting of the data [62]. Bagali et al. utilised the pseudo steam of banana-based activated carbon for Pb(II) ion removal using batch mode process and investigated the kinetics for the adsorption process by altering operating variables [63]. The authors stated that the capacity of adsorption to be 34.21 mg/g and pseudo 2nd order kinetics model demonstrated the best fitting of the data.

3.4. Adsorption isotherm modelling

Equilibrium isotherms are functionalised in order to develop systems for the adsorption process and recitation relation between the capacity of adsorption/desorption and adsorbate [64]. The well-known isotherms models of Langmuir and Freundlich were used to fully comprehend the adsorbate particle distribution between the adsorbent and the liquid, depending on various assumptions mostly related to adsorbent homogeneity or heterogeneity, the likelihood of interaction method, and coverage between several adsorbate particles [6].
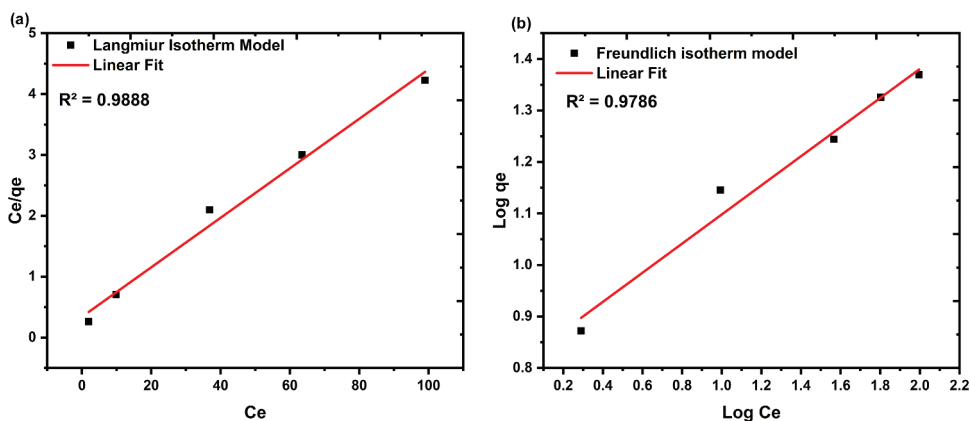
Figure 3. Isotherm model of (a) Langmuir model and (b) Freundlich model for removal of Pb(II) ions via MATSAC.
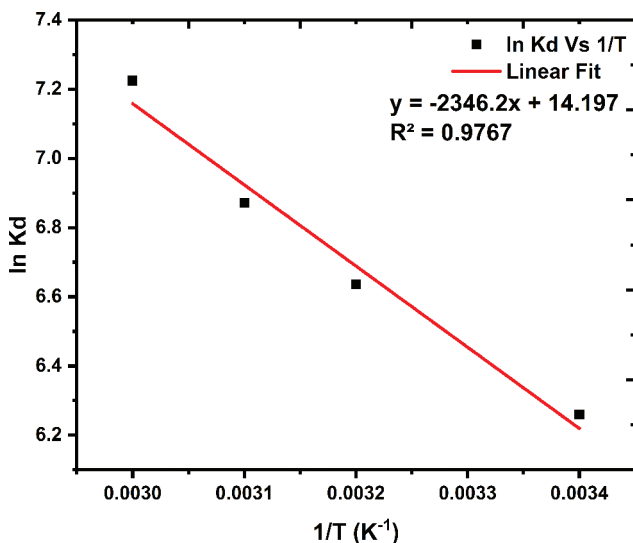
3.4.1. Langmuir isotherm

The Langmuir model has found on the postulation that the highest adsorption happens as soon as enough monolayer of solute particles exists on the adsorbent surface, keeping constant the adsorption energy, which means identical over all areas and there is not any migration of absorbable particles in the plane of the surface [65]. These are comparably better models of isotherm in explaining the adsorption of chemicals [65]. The suitability of this model can be examined through the plot of specific adsorption (C_e/q_e) versus the concentration of equilibrium (C_e) as the linear in Figure 3(a). The unknown value of constraints namely the adsorption energy (b) and the highest capacity of adsorption (q_{max}) can be measured from the intercept and slope of the plot given [66] (Table 4).

3.4.2. Freundlich isotherm

One of the adsorption isotherms employed for liquids to pronounce adsorption on a surface possessing the heterogeneous energy distribution is the Freundlich isotherm. Freundlich isotherm is derived assuming heterogeneity surface and presented in a logarithmic scale using the expression. The suitability of the isotherm was verified via the equation (Equation (10)) of the Freundlich model, which is linearised. Freundlich constants (1/n and K_f) values can be obtained through the ln q_e versus ln C_e plot (Figure 3(b)), and their values are given in Table 4.

Table 4. Parameters of Langmuir and Freundlich isotherms for Pb(II) ion adsorption by MATSAC and other adsorbents.

Adsorbent	Langmuir			Freundlich			References
	q_{max}	b	R^2	K_f	n	R^2	
MATSAC	24.57	0.119	0.9888	6.539	3.537	0.9786	Current study
FSAC	80.64	0.112	0.996	13.86	2.557	0.947	[44]
activated tea waste	1.351	0.789	0.9995	1.801	2.010	0.9853	[67]
Maize tassel based activated carbon	37.31	0.062	0.9997	0.077	0.482	0.9515	[68]
Groundnut shell	4.264	0.062	0.9554	0.3581	1.631	0.9098	[47]

**Figure 4.** Fitting of adsorption data to the plot of $\ln(K_d)$ *vs* [1/T].

The outcomes given in Figure 3 discovered that a higher R^2 (0.9888) was detected on the isothermal model of Langmuir (Table 4). This indicates that Langmuir is more suitable to describe Pb(II) ion adsorption by MATSAC. From the result, it can be concluded that the active sites of MATSAC were regularly dispersed and the monolayer adsorption via chemical adsorption is achieved.

3.5. Thermodynamics study

In this study, a plot of $\ln K_d$ *vs* [1/T] as shown in Figure 4 was generated. From the plot, the value of ΔS and ΔH was detected from the intercept and slope, respectively. The obtained values of thermodynamic parameters are presented in Table S6. From the results, the change in enthalpy value was observed to be positive, which showed that the biosorption reaction is endothermic due to the increase in biosorption upon the consecutive increase in the temperature. The negative value of ΔG revealed that the adsorption reaction by MATSAC is thermodynamically spontaneous. The enhanced randomness at the solid-solution interface during the biosorption of the chromium ion on the active sites of the bio-sorbent is shown by a positive value of ΔS.

3.6. Desorption study of MATSAC

Figure 5 displays the MATSAC routine of the HCl and HNO3 desorption. It was discovered that the desorption increased with eluent concentration until a specific limit was reached. For HCl and HNO_3, this concentration was recorded at 4 M. It was discovered that the desorption could not be greatly boosted over this concentration limit. HNO_3 had greater desorption efficiency than HCl, even though both eluents displayed a nearly identical pattern of desorption. This investigation has shown that utilising HNO_3 at a concentration of 6 M resulted in the greatest desorption of 77% of Pb(II) ions. It is also well established
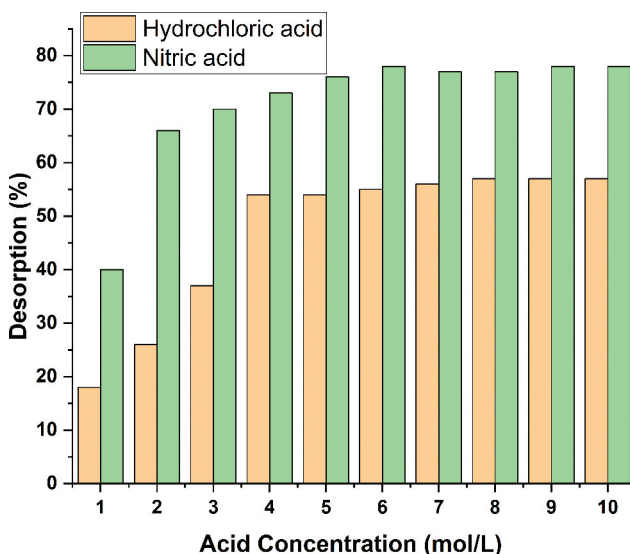
Figure 5. Desorption of Pb(II) ions from MATSAC with respect to different concentrations of hydrochloric acid and nitric acid.

that even the use of more concentrated HCl or HNO_3 could not result in the complete desorption of Pb(II) ions from the MATSAC surface. In the end, it was also discovered that the adsorption process is reversible.

4. Conclusions

Teff (*Eragrostis tef*) is an annual grass native to the Horn of Africa, particularly Ethiopia. This work aimed to prepare teff straw-based activated carbon (MATSAC) and examine the adsorption potential of Pb(II) ions. The prepared MATSAC was characterised by the techniques, namely, FTIR, XRD, SEM, BET, and P_{ZC}. Batch adsorption studies were carried out using TSAC to optimise crucia independent factors such as initial Pb(II) ion concentration, MATSAC dose, pH, and contact time using RSM. It was statistically optimised to achieve the maximum removal (90.89%) of Pb(II) ions at 94.35 mg/L, 0.655 g/100 mL, 87.6 min, and 5.4 for initial Pb(II) ions concentration, MATSAC dose, adsorption time and solution pH, respectively. Isotherm studies explicated that the Langmuir isotherm was found to be better appropriate with a high correlation coefficient than the Freundlich isotherm. In the kinetic analysis, it was clear that the rate of adsorption of Pb(II) ions on the MATSAC was observed to be better suited by a pseudo-second-order model. The parameters of thermodynamic obtained showed that the adsorption of the Pb(II) ions on MATSAC is spontaneous and endothermic. In a nutshell, MATSAC that is developed from a locally obtainable waste of agriculture can be a cheap and potential adsorbent that can remove Pb(II) ions from contaminated water.

Disclosure statement

ORCID

Surafel Mustefa Beyan 🅳 http://orcid.org/0000-0002-3288-7748

References

[1]   U.N.W.W.A.P. WWAP, *The United Nations World Water Development Report 2017. Wastewater: The Untapped Resource* (UNESCO, Paris, 2017).

[2]   G. Azeh Engwa, P. Udoka Ferdinand, F. Nweke Nwalo and M. NMechanism and Health Effects of Heavy Metal Toxicity in Humans, *Poisoning Mod. World - New Tricks an Old Dog?* London, United Kingdom: BoD 77–100, (2019).

[3]   A. Ishaque, L. Johnson, T. Gerald, D. Boucaud, J. Okoh and P. Tchounwou, Int. J. Environ. Res. Public Health. **3**, 118 (2006). doi:10.3390/ijerph2006030014.

[4]   E. Koohzad, D. Jafari and H. Esmaeili, ChemistrySelect **4**, 12356 (2019). doi:10.1002/slct.201903167.

[5]   M. Kaur, S. Kumari and P. Sharma, Biotechnol. Reports. **25**, e00410 (2020). doi:10.1016/j.btre.2019.e00410.

[6]   Y. Asrat, A.T. Adugna, M. Kamaraj and S.M. Beyan, J. Chem. **2021**, 1 (2021). doi:10.1155/2021/5554353.

[7]   S.M. Beyan, S.V. Prabhu, T.T. Sissay and A.A. Getahun, Bioresour. Technol. Reports. **14**, 100664 (2021). doi:10.1016/j.biteb.2021.100664.

[8]   S. Liang, X. Guo, N. Feng and Q. Tian, J. Hazard. Mater. **174**, 756 (2010). doi:10.1016/j.jhazmat.2009.09.116.

[9]   C. Tejada-Tovar, A.D. Gonzalez-Delgado and A. Villabona-Ortiz, Appl. Sci. **9**, 4486 (2019). doi:10.3390/app9214486.

[10] D. Berihun and J. Mater, Sci. Eng. **6**, 6 (2017).

[11] V.K.G. Suhas, P.J.M. Carrott, R. Singh, M. Chaudhary and S. Kushwaha, Bioresour. Technol. **216**, 1066 (2016). doi:10.1016/j.biortech.2016.05.106.

[12] P.J.M.C. Suhas and M.M.L. Ribeiro Carrott, Bioresour. Technol. **98**, 2301 (2007). doi:10.1016/j.biortech.2006.08.008.

[13] B. Heibati, S. Rodriguez-Couto, M.A. Al-Ghouti, M. Asif, I. Tyagi, S. Agarwal and V.K. Gupta, J. Mol. Liq. **208**, 99 (2015). doi:10.1016/j.molliq.2015.03.057.

[14] M. Verma, I. Tyagi, R. Chandra and V.K. Gupta, J. Mol. Liq. **225**, 936 (2017). doi:10.1016/j.molliq.2016.04.045.

[15] Y. Abshirini, H. Esmaeili and R. Foroutan, Mater. Res. Express. **6**, 125513 (2019). doi:10.1088/2053-1591/ab56ea.

[16] T. Khedri and H. Esmaeili, J. Dispers. Sci. Technol. **1**, 1–12 (2021). doi:10.1080/01932691.2021.2013869.

[17] A. Asfaram, M. Ghaedi, G.R. Ghezelbash, E.A. Dil, I. Tyagi, S. Agarwal and V.K. Gupta, J. Mol. Liq. **214**, 249 (2016). doi:10.1016/j.molliq.2015.12.075.

[18] A.M. Ghaedi, M. Ghaedi, A. Vafaei, N. Iravani, M. Keshavarz, M. Rad, I. Tyagi, S. Agarwal and V.K. Gupta, J. Mol. Liq. **206**, 195 (2015). doi:10.1016/j.molliq.2015.02.029.

[19] S.P. Boeykens, N. Redondo, R.A. Obeso, N. Caracciolo and C. Vázquez, Appl. Radiat. Isot. **153**, 108809 (2019). doi:10.1016/j.apradiso.2019.108809.

[20] T.A. Amibo, S.M. Beyan and T.M. Damite, Adv. Mater. Sci. Eng. **2021**, 1 (2021). doi:10.1155/2021/9444577.

[21] T.A. Amibo, S.M. Beyan, M. Mustefa, P.S. Venkatesa and A.B. Bayu, Mater. Res. Innov. **25**, 1–10 (2021). doi:10.1080/14328917.2021.2022372.

[22] H. Esmaeili and S. Tamjidi, Environ. Sci. Pollut. Res. **27**, 31652 (2020). doi:10.1007/s11356-020-09448-y.

[23] M.J. Puchana-Rosero, M.A. Adebayo, E.C. Lima, F.M. Machado, P.S. Thue, J.C.P. Vaghetti, C.S. Umpierres and M. Gutterres, Colloids Surfaces A Physicochem. Eng. Asp. **504**, 105 (2016). doi:10.1016/j.colsurfa.2016.05.059.

[24] D.C. Dos Santos, M.A. Adebayo, S. de Fátima Pinheiro Pereira, L.D.T. Prola, R. Cataluña, E. C. Lima, C. Saucier, C.R. Gally and F.M. Machado, Korean J. Chem. Eng. **31**, 1470 (2014). doi:10.1007/s11814-014-0086-3.

[25] A.I. Osman, J. Blewitt, J.K. Abu-Dahrieh, C. Farrell, A.H. Al-Muhtaseb, J. Harrison and D. W. Rooney, Environ. Sci. Pollut. Res. **26**, 37228 (2019). doi:10.1007/s11356-019-06594-w.

[26] A. Shahat, H.M.A. Hassan, H.M.E. Azzazy, E.A. El-Sharkawy, H.M. Abdou and M.R. Awual, Chem. Eng. J. **332**, 377 (2018). doi:10.1016/j.cej.2017.09.040.

[27] L.P. Cruz-Lopes, M. Macena, B. Esteves and R.P.F. Guiné, Open Agric. **6**, 115 (2021). doi:10.1515/opag-2021-0225.

[28] O.S. Bello, K.A. Adegoke and O.O. Akinyunni, Appl. Water Sci. **7**, 1295 (2017). doi:10.1007/s13201-015-0345-4.

[29] S.R. Singh and A.P. Singh, Int. J. Environ. Res. **6**, 917 (2012).

[30] M. Dizbay-Onat, U.K. Vaidya, J.A.G. Balanay and C.T. Lungu, Adsorpt. Sci. Technol. **36**, 441 (2018). doi:10.1177/0263617417700635.

[31] F. Kebede and G. Alemayehu, Open Access J. Sci. Technol. **5**, 1 (2017). doi:10.11131/2017/101214.

[32] A.R. Hidayu, N.F. Mohamad, S. Matali and A.S.A.K. Sharifah, Procedia Eng. **68**, 379 (2013). doi:10.1016/j.proeng.2013.12.195.

[33] P. Senthil Kumar, G.J. Joshiba, C.C. Femina, P. Varshini, S. Priyadharshini, M.S. Arun Karthick and R. Jothirani, Desalin. WATER Treat. **172**, 395 (2019). doi:10.5004/dwt.2019.24613.

[34] D. Mihayo, M.R. Vegi and S.A.H. Vuai, Adsorpt. Sci. Technol. **2021**, 1 (2021). doi:10.1155/2021/5574900.

[35] M.S. Shamsuddin, N.R.N. Yusoff and M.A. Sulaiman, Procedia Chem. **19**, 558 (2016). doi:10.1016/j.proche.2016.03.053.

[36] H.P.S.A. Khalil, M. Jawaid, P. Firoozian, U. Rashid, A. Islam and H.M. Akil, J. Biobased Mater. Bioenergy. **7**, 708 (2013). doi:10.1166/jbmb.2013.1379.

[37] B. Tesfaw, F. Chekol, S. Mehretie and S. Admassie, Bull. Chem. Soc. Ethiop. **30**, 473 (2017). doi:10.4314/bcse.v30i3.16.

[38] T.K. Mumecha, B. Surafel Mustefa, S. Venkatesa Prabhu and F.T. Zewde, Eng. Appl. Sci. Res. **48**, 171 (2021).

[39] M. Rafatullah, O. Sulaiman, R. Hashim and A. Ahmad, J. Hazard. Mater. **170**, 969 (2009). doi:10.1016/j.jhazmat.2009.05.066.

[40] R. Ahmad and S. Haseeb, Arab. J. Chem. **10**, S412 (2017). doi:10.1016/j.arabjc.2012.09.013.

[41] P. Brown, I. Atly Jefcoat, D. Parrish, S. Gill and E. Graham, Adv. Environ. Res. **4**, 19 (2000). doi:10.1016/S1093-0191(00)00004-6.

[42] T. Anitha, P.S. Kumar, K.S. Kumar, K. Sriram and J.F. Ahmed, Desalin. Water Treat. **57**, 13711 (2016).

[43] E. Khanniri, M. Yousefi, A.M. Mortazavian, N. Khorshidian, S. Sohrabvandi, M. Arab and M. R. Koushki, Int. J. Biol. Macromol. **178**, 53 (2021). doi:10.1016/j.ijbiomac.2021.02.065.

[44] M. Ghasemi, M. Naushad, N. Ghasemi and Y. Khosravi-fard, J. Ind. Eng. Chem. **20**, 454 (2014). doi:10.1016/j.jiec.2013.05.002.

[45] N. Gnanasundaram, M. Loganathan and A. Singh, IOP Conf. Ser. Mater. Sci. Eng. **206**, 012065 (2017). doi:10.1088/1757-899X/206/1/012065.

[46] J. Aravind, P. Kanmani, G. Sudha and R. Balan, Glob. J. Environ. Sci. Manag. **2**, 61 (2016).

[47] J. Bayuo, B. Kenneth and A.A. Moses, Phys. Chem. An Indian J. Res. Artic. **14**, 123 (2019).

[48] S. Tamjidi and H. Esmaeili, Chem. Eng. Technol. **42**, 607 (2019). doi:10.1002/ceat.201800488.

[49] M. Meigoli Boushehrian, H. Esmaeili and R. Foroutan, J. Environ. Chem. Eng. **8**, 103869 (2020). doi:10.1016/j.jece.2020.103869.

[50] M.R. Awual, M.M. Hasan, A. Islam, M.M. Rahman, A.M. Asiri, M.A. Khaleque and M.C. Sheikh, J. Clean. Prod. **231**, 214 (2019). doi:10.1016/j.jclepro.2019.05.125.

[51] M. Abdulkarim and F.A. Al-Rub, Adsorpt. Sci. Technol. **22**, 119 (2004). doi:10.1260/026361704323150908.

[52] V.J.P. Vilar, C.M.S. Botelho and R.A.R. Boaventura, Process Biochem. **40**, 3267 (2005). doi:10.1016/j.procbio.2005.03.023.

[53] H. Esmaeili, S. Tamjidi and M. Abed, Desalin. WATER Treat. **174**, 324 (2020). doi:10.5004/dwt.2020.24880.
[54] R. Foroutan, H. Esmaeili, A.M. Sanati, M. Ahmadi and B. Ramavandi, Desalin. Water Treat. **135**, 236 (2018). doi:10.5004/dwt.2018.23179.
[55] Y. HO, J. Hazard. Mater. **136**, 681 (2006).
[56] P.S. Venkatesa, G. Girma, A.K. Gizachew, B.M. Surafel and R. G, Int. J. Recent Technol. Eng. **8**, 4808 (2019).
[57] S. Venkatesa Prabhu, G. Ramesh, A.T. Adugna, S.M. Beyan and K. Gizachew Assefa, Int. J. Innov. Technol. Explor. Eng. **8**, 76 (2019).
[58] U.R. Lakshmi, V.C. Srivastava, I.D. Mall and D.H. Lataye, J. Environ. Manage. **90**, 710 (2009). doi:10.1016/j.jenvman.2008.01.002.
[59] X.S. Wang, Z.Z. Li and S.R. Tao, J. Environ. Manage. **90**, 721 (2009). doi:10.1016/j.jenvman.2008.01.011.
[60] V.S. Mane, I. Deo Mall and V. Chandra Srivastava, J. Environ. Manage. **84**, 390 (2007). doi:10.1016/j.jenvman.2006.06.024.
[61] J. Huang, Y. Cao, Z. Liu, Z. Deng, F. Tang and W. Wang, Chem. Eng. J. **180**, 75 (2012). doi:10.1016/j.cej.2011.11.005.
[62] B.G. Alhogbi, Sustain. Chem. Pharm. **6**, 21 (2017). doi:10.1016/j.scp.2017.06.004.
[63] S.S. Bagali, B.S. Gowrishankar and A.S. Roy, Engineering **3**, 409 (2017). doi:10.1016/J.ENG.2017.03.024.
[64] F. Takmil, H. Esmaeili, S.M. Mousavi and S.A. Hashemi, Adv. Powder Technol. **31**, 3236 (2020). doi:10.1016/j.apt.2020.06.015.
[65] L. Liu, Y. Rao, C. Tian, T. Huang, J. Lu, M. Zhang and M. Han, Adsorpt. Sci. Technol. **2021**, 1 (2021). doi:10.1155/2021/7189639.
[66] A.Q. Alorabi, Adsorpt. Sci. Technol. **2021**, 1 (2021). doi:10.1155/2021/2359110.
[67] M.K. Mondal, Korean J. Chem. Eng. **27**, 144 (2010). doi:10.1007/s11814-009-0304-6.
[68] M. Moyo, L. Chikazaza, B.C. Nyamunda and U. Guyo, J. Chem. **2013**, 1 (2013). doi:10.1155/2013/508934.